ORIGINAL ARTICLE Musculoskeletal Imaging

Can T2* relaxation time be considered as an alternative bone structural index?

Panagiotis Tsialios[1], Efstratios Karavasilis[1], Konstantinos Stathopoulos[2], Odysseas Benekos[3], Georgios Velonakis[1], Grigorios Skarantavos[4], Efstathios Efstathopoulos[1]

[1]Second Department of Radiology, Attikon University Hospital, Medical School, National and Kapodistrian University, Athens, Greece

[2]National and Kapodistrian University of Athens, School of Medicine, Postgraduate course on Bone Metabolic Diseases, Athens, Greece

[3]Philips Hellas SA, Chalandri, Athens, Greece

[4]First University Orthopaedic Clinic, Attikon University Hospital, Athens, Greece

ABSTRACT

Purpose: The aim of this study was to assess the skeletal status in postmenopausal women evaluating the correlation between active transverse relaxation time T_2^* as measured by Magnetic Resonance Imaging (MRI), and areal or apparent volumetric bone mineral density respectively as measured by Dual energy X-ray Absorptiometry (DXA) and peripheral quantitative computed tomography.

Material and Methods: T_2^* relaxation times of the lumbar spine and tibia were estimated in 8 postmenopausal osteoporotic women [mean age: 64.9 ± 7.8 (1 S.D.) years] scanned in a 3.0 T MRI scanner, 5 postmenopausal osteoporotic women [mean age: 68.4 ± 9.1 (1 S.D.) years] scanned in a 1.5 T MRI scanner and 5 female healthy volunteers [mean age: 33.3 ± 10.4 (1 S.D.) years], scanned in both MRI scanners. Both patient and control groups performed peripheral Quantitative Computed Tomography (pQCT) of the tibia and DXA of the lumbar spine. T-test statistical analyses were performed to identify changes of measured bone density parameters and calculated T_2^* relaxation times between patient and healthy controls. In addition, correlations between

CORRESPONDING AUTHOR, GUARANTOR

Corresponding author: Panagiotis Tsialios, Second Department of Radiology, Attikon University Hospital, Medical School, National and Kapodistrian University, 27 P. Grigoriou & Neapoleos Str, Ayia Paraskevi, 15341 Athens, Greece, Email: ptsialios@gmail.com

Guarantor: Efstathios Efstathopoulos, Second Department of Radiology, Attikon University Hospital, Medical School, National and Kapodistrian University, 1 Rimini Str, Chaidari, 12462 Athens, Greece, Email: stathise@med.uoa.gr

bone mineral density parameters and T_2^* relaxation time were estimated.

Results: Patients showed reduced bone mineral density parameters in both lumbar spine and tibia compared to controls. Additionally, correlation factors between T_2^* relaxation times and measured bone density parameters (Bone Mineral Density-BMD, volumetric BMD-vBMD and

trabecular volumetric density-TrD) were found significant, ranging between r=-0.58 (p<0.05) to r=-0.87 (p<0.05) for both MRI scanners.

Conclusions: T_2^* measurements could possibly assess changes in bone status related to BMD measurements between healthy premenopausal and osteoporotic postmenopausal women.

KEY WORDS

Magnetic resonance imaging; T_2^* mapping; Dual energy x-ray absorptiometry; pQCT; Postmenopausal osteoporosis; Bone density

Introduction

Fragility fractures in patients with compromised bone strength, either suffering from osteoporosis or other bone metabolic diseases, constitute a significant medical, social and economic burden worldwide. In 2010, 3.5 million fractures were estimated in the European Union and the cost of osteoporosis was estimated at 37 billion euros, of which 66% were costs of treating fractures [1].

Although Dual energy X-ray Absorptiometry (DXA) is considered the gold standard for the diagnosis of osteoporosis, it has been shown that it cannot provide a threshold for the estimation of fracture risk alone as, indeed, the majority of osteoporotic fractures has been recorded in patients with osteopenia rather than osteoporosis [2]. Bone Mineral Density (BMD) as measured by DXA estimates milligrams of hydroxyapatite per cm² of projected bone area (thus, the resulting measurement is significantly dependent on bone size) and has been shown to account for approximately 2/3 (66%) of bone strength of isolated bones in vitro [1]. However, DXA does not possess the discerning ability to differentiate between trabecular and cortical bone [3], so that independent contributions of each compartment in bone strength cannot be assessed. Moreover, the parameters of microarchitecture (i.e. trabecular thickness, number and connectivity, cortical thickness and cortical porosity) are not captured by DXA [4-8]. As a result, other techniques for non-invasive estimation of bone strength parameters are currently needed in order to assist in the prediction of future fracture. One of them, already being used in various clinical settings around the world, is peripheral Quantitative Computed Tomography (pQCT).

This technique, performed at peripheral skeletal sites such as the radius and tibia, has the ability to differentiate between the trabecular and cortical compartment of bone and it is used to estimate volumetric BMD (vBMD, mg/cm³) as well as geometrical parameters such as cross sectional areas (mm²) of trabecular, subcortical and cortical bone, periosteal and endosteal circumference (mm) and provides also indicators of bending and torsional strength (stress strength index, SSI) with good reproducibility, precision and accuracy [9].

Clinical and experimental studies have shown that MRI has also the potential to be a useful method for the study of trabecular bone [10-13]. The technical background of this method can be explained by the differences in the magnetic susceptibilities between the inter-surfaces of trabecular bone and bone marrow, leading to spatial inhomogeneities of the magnetic field. T_2^* relaxation time comprises a characteristic parameter of each tissue, that is dependent on molecular interaction (T_2 relaxation time) and on inhomogeneities of the magnetic field, as seen in Equation 1. Therefore, T_2^* alterations can provide information about the structure and the density of the spongy osteal plexus [14]. Additionally, T_2^* measurements have been performed at several skeletal sites with high trabecular content such as the spine, proximal femur and calcaneus, providing adequate information concerning both structure and density of the trabecular compartment of bone [15-18]. To the best of our knowledge, there are merely two published studies that had estimated the bone structural integrity using DXA, pQCT and high resolution MRI [19, 20]. This is the first study which compares two ionising techniques, DXA and pQCT,

with a non-ionising technique, T_2^* relaxometry using two different magnetic field MRI systems in two different anatomical areas, lumbar spine and tibia.

The aim of the study, which is a hypothesis-generating study, was to assess T_2^* relaxation time as a potential index to characterise the bone structural integrity. More precisely, a) to examine the efficiency of T_2^* measurements to discriminate women with and without osteoporotic trabecular bone architecture and b) to estimate the correlation between T_2^* and established bone structural indices, BMD, trabecular and total vBMD.

Equation 1

$$\frac{1}{T_2^*} = \frac{1}{2T_1} + \frac{1}{T_2} + \frac{\gamma \Delta B}{2}$$

where T_2 is the true transverse relaxation time and T_1 is the longitudinal relaxation time, both reflecting signal decay in a perfectly homogeneous magnetic field. T_2^* is the effective T_2 relaxation time, γ is the gyromagnetic ratio and ΔB is the magnetic field inhomogeneity across a voxel. It is worth noting that in normal clinical conditions the term $\frac{1}{2T_1}$ is always smaller than the term $\frac{1}{T_2}$ and far smaller than the apparent term $\frac{\gamma \Delta B}{2}$. Practically, the term $\frac{1}{2T_1}$ is negligible and will not importantly affect the total sum for the final calculation of T_2^*.

Material and Methods
Clinical Study

In our study, 13 osteoporotic postmenopausal women (defined by DXA T-score-2.5 at the spine, >1 year menopause), without medical history of previous tibia fracture, recent immobilisation or other medical conditions known to affect bone strength, were randomly allocated into 2 groups (group A=5 patients and group B=8 patients). A third group of 5 healthy women was used as a control (group C). All subjects provided written informed consent, and the study was approved by the ethics committees of both "Attikon" Athens University General Hospital and KAT General Hospital of Athens.

All the participants underwent pQCT of the tibia, as well as DXA and MRI of the lumbar spine. All measurements were performed within 7-10 days so as to minimise biological differences between them. Group A was scanned in a 1.5 T scanner and group B in a 3.0 T scanner. Control group

C was scanned in both systems to evaluate the deviations of T_2^* between 1.5 T and 3.0 T magnetic fields.

Bone mineral density measurements

All the participants were scanned in the same DXA and pQCT scanners. BMD measurements were obtained on L_1-L_4 vertebrae in anteroposterior projections using DXA scanner Lunar Prodigy Pro (GE Healthcare, Madison, USA).

Tibia pQCT measurements were performed using the Stratec XCT-3000 scanner (StratecMedizintechnik GmbH) according to the following acquisition protocol [21]. Initially, tibia length (cm) was estimated measuring the distance between the medial malleolus and medial tibial plateau. Then, 3 slices were obtained at the 4%, 14% and 38% of tibial length sites. The 4% site represents the trabecular bone, the 14% cortical and subcortical bone and the 38% cortical bone. At the 4% site, we estimated total vBMD and trabecular volumetric density (TrD) for all subjects. The accuracy and reproducibility of measurements were calculated in a separate analysis as coefficient of variation (%CV) and was found to be between 0.3–0.6% for trabecular and cortical BMD.

MR phantom study

Prior to patient examinations, measurements of solutions at different concentrations of paramagnetic agent (gadolinium diethylenetriaminepentaacetic acid Gd-DTPA, Magnevist™, Bayer HealthCare Pharmaceuticals Inc., Germany) were performed in order to evaluate the MRI protocol's accuracy and estimate the T_2^* variation, in conjunction with the increase of gadolinium concentration, in both MRI systems of 1.5 T and 3.0 T.

Fifteen Gd-doped deionised water solutions with Gd concentration ranging from 1 mM to 15 mM and one 30 ml vial of clear deionised water were prepared. Each Gd-DTPA solution was positioned in a 30 ml polycarbonate cylindrical vial (diameter 2.7 cm and length 8 cm) placed in a case made of Plexiglas as seen in **Fig. 1**, and stored in the magnet room for 24 h prior to measurements for temperature stabilisation. Throughout the phantom study, the solutions temperature was 22 ± 1 °C. The vials were positioned parallel to the main magnetic field to minimise distortions due to the inhomogeneity of the magnetic field. The phantom was scanned twice in both scanners increasing the Num-

Table 1. Basic parameters of the sequences, for both MRI scanners.				
	MRI 3.0 T		**MRI 1.5 T**	
	Spine	**Tibia**	**Spine**	**Tibia**
First TE (ms)	2.3	1.34	2.3	1.9
ΔTE (ms)	2.3	2.3	4.6	4.6
TR (ms)	535	284	82	147
Flip Angle	30°	30°	30°	30°
Reconstruction voxel (mm)	1.29/1.30/4	1.17/1.19/4	0.78/0.78/5	0.59/0.59/5
Gap (mm)	0.4	0.4	0.5	0.5
Number of echoes	20	20	25	25
Bandwidth (Hz/pixel)	438	432	427	424
Imaging orientation	Sagittal	Axial	Sagittal	Axial

ber of Signal Averages (NSA) in order to increase the signal-to-noise ratio (SNR) of the last TEs. The mean percentage of the SNR increase was calculated at the level of 3%. Assuming that the signal decay is not impaired from this slight increase of SNR, we calculated the %CV in order to estimate the repeatability of our T_2^* measurements.

Quality assurance (QA) tests were performed to assess both MRI systems' performance, including magnetic field homogeneity, geometric accuracy, artefact evaluation, slice thickness accuracy, slice positioning and alignment accuracy, image uniformity and SNR for the used multi-channel received RF coils. The aforementioned procedure has been described in details by Price et al. [22].

T_2^* measurements

T_2^* measurements in both lumbar spine and tibia were estimated using body RF surface coil and ankle volume coil at 1.5 T Intera (Philips Healthcare, Best, The Netherlands) and 3.0 T Achieva TX (Philips Healthcare, Best, The Netherlands) MRI scanners. A series of conventional gradient echo T_1-weighted imaging sequences were applied as surveys in axial, sagittal and coronal planes in order to locate the lumbar region of the spine and the 4% of the length of the tibia from the lower articular surface. The clinical used lumbar spine imaging proto-

col consisted of T_1 and T_2 Turbo Spin Echo (TSE) in axial and sagittal plane and T_2 Inversion Recovery (STIR) in the sagittal plane. No clinical protocol was applied in the tibia.

Gradient multi echo, multi slice sequences (mFFE) were applied in sagittal and axial plane to the lumbar spine and the tibia, respectively for the quantitative estimation of T_2^*. Twenty and twenty-five echoes were acquired in 3.0 T and 1.5 T MRI scanners, respectively in order to have numerous points to achieve better fitting. Moreover, the echo spacing, ΔTE, was 2.3 ms and 4.6 ms for 3.0 T and 1.5 T MRI systems, respectively in order to obtain data exclusively in in- or out-phase, and to avoid the sinusoidal signal decay due to the water fat chemical shift phaenomenon. Furthermore, receiver bandwidth was set about 400 Hz/pixel to minimise the geometric distortions and severe susceptibility artefacts. Acquisition parameters of the sequences for both MRI scanners are presented in detail in **Table 1**.

Region of interests (ROIs) were drawn in the central slice corresponding to 4% of the length of the tibia from the lower articular surface and in the central slices of lumbar vertebrae L_1–L_4. ROIs were also drawn to an artefact-free area in the background of the acquired image and parallel to the phase encoding axis. The measured background values were subtracted from the actual signal measured in tibia and vertebra.

Fig. 1. Fifteen 30 ml polycarbonate cylindrical vials containing Gd-doped deionised water solutions with Gd concentration ranging from 1 mM to 15 mM and one 30 ml vial of clear deionised water (upper left) were mounted in a Plexiglas case.

The calculated with the corresponding TE values were imported into MATLAB R2018b (Mathworks, USA) software and then, using Levenberg-Marquardt method [23], T_2^* times were estimated, according to Equation 2. The above methodology was also applied in the phantom study.

Equation 2

$$S'(TE) = S(TE) - Bg = S_0 exp\left(-\frac{TE}{T_2^*}\right)$$

where TE is the echo time, S is the signal intensity and Bg is the background noise.

Statistical Methods
Authors have firstly checked if the normal distribution model fits the calculated parameters using the Shapiro-Wilk tests. The data were normally distributed, therefore unpaired parametric Student's t-test analyses were performed to identify statistical significant differences of both measured bone density parameters (BMD, vBMD and TrD) and calculated T_2^* relaxation times between patient and healthy controls. In addition, correlations between measurable bone density parameters and T_2^* relaxation times were estimated by means of normal linear regression analysis amongst study groups. All statistical analyses were conducted

via the Statistical Package for Social Sciences (SPSS v25, Chicago, U.S.A.).

Results
Two of the 20 women who were initially included in the study were excluded after the initial evaluations resulting in 18 women remaining in the study. One woman was suffering from severe scoliosis and extensive spondyloarthritis, thereby not permitting an accurate evaluation of her BMD by DXA. Artefacts due to the above factors are more common in the lumbar spine, especially in the older population [24, 25]. The second woman suffered a panic attack while undertaking the MRI examination, probably caused by claustrophobia, and therefore withdrew from the study. Anthropometric variables such as age, height and mass were recorded and body mass index (BMI) was calculated for all subjects as seen in **Table 2**.

Phantom Study
Table 3 depicts the measurements performed in vials of different gadolinium concentration using both MRI systems.

T_2^* decreases when gadolinium concentration increases in both MRI scanners, according to the following equations:

$T_2^* = 128.01x^{-0.86}$ (*Equation 3*), (R^2 = 0.995) on 1.5 T and
$T_2^* = 150.44x^{-0.98}$ (*Equation 4*), (R^2 = 0.995) on 3.0 T, respectively.

Also, T_2^* times are shown to be shorter on 3.0 T compared to 1.5 T, as expected [26]. The calculated %CV ranged from 0.10% to 1.18% and from <0.1% to 1.45% in 1.5 T and 3.0 T, respectively.

Clinical Study
Table 4 depicts measured (BMD, vBMD, TrD) and calculated (T_2^* relaxation times) quantitative bone structural indices for all studied groups as well as the group statistical comparisons. BMD in the four vertebrae of the lumbar spine as well as vBMD and TrD tibia's density parameters were statistically different between the control group and both postmenopausal groups. In the same pattern, the calculated MR relaxometry parameters showed statistically significant differences between the control group and patient groups **(Fig. 2)**.

Correlations amongst measurable BMD parameters and calculated T_2^* relaxation times were performed by

Table 2. Anthropometric variables between groups.			
Parameter/Group	A (n=5)	B (n=8)	C (n=5)
Age (y)	68.4 ± 9.1	64.9 ± 7.8	33.3 ± 10.4
Mass (kg)	66.9 ± 9.6	64.6 ± 10.8	64.1 ± 10.5
Height (cm)	155.1 ± 5.5	153.9 ± 4.6	162.3 ± 5.9
BMI (kg/m^2)	27.7 ± 3.8	27.2 ± 3.5	24.4 ± 4.4

BMI: Body mass index.

Data are mean ± standard deviation.

Table 3. Signal vial's ROIs measurements in both MRI scanners.						
Concentration (mmol/L)	T_2* relaxation time (1.5 T) (ms)			T_2* relaxation time (3.0 T) (ms)		
	mFFE (ΔTE=2.3 ms NSA=2)	mFFE (ΔTE=2.3 ms NSA=6)	%CV	mFFE (ΔTE=3 ms NSA=1)	mFFE (ΔTE=3 ms NSA=10)	%CV
H_2O vial	386.74	393.23	1.18	423.11	431.86	1.45
1	127.32	128.83	0.84	149.70	150.48	0.37
2	62.78	63.48	0.78	81.54	81.55	<0.1
3	51.94	51.75	0.26	57.18	56.75	0.52
4	38.33	38.62	0.53	34.27	34.42	0.31
5	35.41	34.95	0.92	29.72	29.83	0.24
6	28.99	29.09	0.23	24.82	24.91	0.23
7	25.17	24.91	0.73	21.72	21.80	0.24
8	22.97	23.01	0.10	19.88	19.88	<0.1
9	19.60	19.80	0.75	17.47	17.47	<0.1
10	17.62	17.74	0.46	16.16	16.17	<0.1
11	16.42	16.49	0.29	15.09	15.08	<0.1
12	15.01	15.21	0.92	13.58	13.57	<0.1
13	13.85	14.07	1.13	12.25	12.26	<0.1
14	12.93	12.96	0.10	11.60	11.61	<0.1
15	11.82	11.92	0.56	11.18	11.21	0.10

mFFE: merged Fast Field Echo, ΔTE: the time difference between two echoes, ms: milliseconds and NSA: Number of Signal Averages.

means of normal linear regression analysis. Mean T_2* times showed significant negative associations with mean subjects' BMD, vBMD and TrD parameters ranging from r=-0.58 up to r=-0.87 (p<0.05) **(Fig. 3)**.
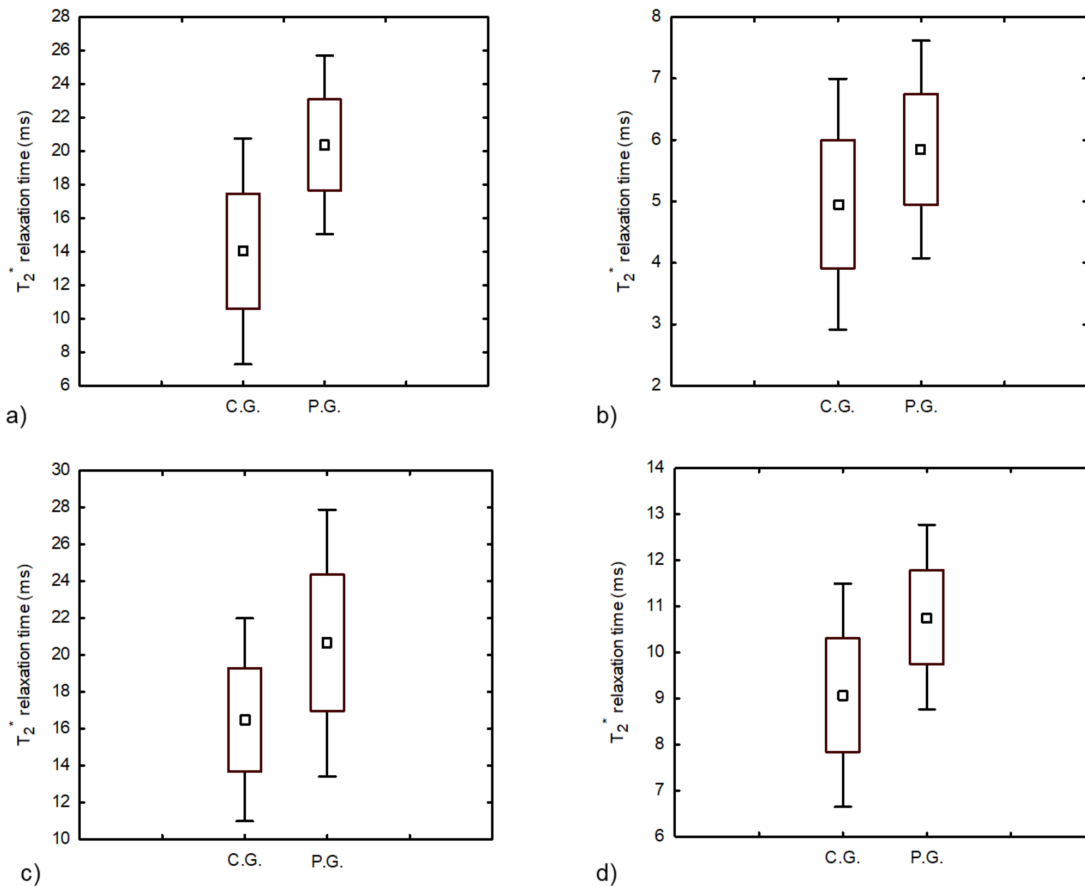
Fig. 2. T_2^* relaxation time changes, between Control Group (C.G.) and Patients Group (P.G.) for both MRI scanners [Lumbar spine: 1.5T **(a)** and 3.0T **(b)**, Tibia: 1.5T **(c)** and 3.0T **(d)**]. (Note ▫ Mean, □ Mean ± SE, Mean ± 1.96*SE).

Discussion

In the present study, we examined the association of T_2^* not only with aBMD of the spine and tibia but also with vBMD parameters of the tibia, which provide volumetric densities of each compartment (trabecular vs. cortical) of the bone and are considered strong determinants of bone strength. Thereafter, a possible significant correlation between T_2^* and volumetric bone density parameters enhances the prognostic value of T_2^* as an alternative bone mineral density biomarker. MRI has been proposed as a new tool, without ionising radiation, for non-invasive assessment of skeletal status in osteoporotic patients. The technical background of this method can be explained by the differences in the magnetic susceptibilities between the inter-surfaces of trabecular bone and bone marrow, leading to spatial inhomogeneities of the magnetic field. These inhomogeneities result in additional dephasing of transverse magnetisation. The change in T_2^* together with the characteristics of this relaxation time provide

information on the density and structure of trabecular bone matrix [17, 27, 28].

T_2^* measurement is an experimental technique that has been investigated in vivo only in a preliminary stage. In this work, we studied the in vivo measurement of T_2^* in two anatomical regions, lumbar spine and 4% of the tibia length from the lower articular surface. These parts of the human skeleton consist mainly of spongy bone and constitute two important anatomical regions to assess BMD changes and osteoporotic fracture risk.

The construction of the MRI phantom allowed us to measure the variation of T_2^* in conjunction with the increase of the gadolinium solutions' concentration. Therefore, it was possible to estimate the measurement limits of the two MRI systems, in order to evaluate the magnetic resonance sequences that would be applied in the clinical part of the experiments as well as the range of values of the relaxation times for which measurements would be unreliable. T_2^* relaxation times were decreased

Table 4. Bone mineral density measurements.

Parameters/ Group	A (n=5)	B (n=8)	C (n=5) 1.5 T	C (n=5) 3.0 T	A vs C (t, p)	B vs C (t, p)
BMD (g/cm²) L1-L4	837.2 ± 68.5 (W=0.82, p=0.14)*	948.3 ± 47.3 (W=0.87, p=0.16)*	1333.2 ± 72.3 (W=0.94, p=0.83)*		t=4.98, p<0.05	t=4.67, p<0.05
vBMD (mg/cm³)	201.7 ± 17.1 (W=0.85, p=0.25)*	235.2 ± 14.6 (W=0.90, p=0.33)*	314.5 ± 16.3 (W=0.95, p=0.91)*		t=4.78, p<0.05	t=3.51, p<0.05
(TrD) (mg/cm³)	145.8 ± 19.4 (W=0.89, p=0.42)*	184.9 ± 10.8 (W=0.93, p=0.57)*	233.9 ± 11.8 (W=0.86, p=0.27)*		t=3.88, p<0.05	t=2.95, p<0.05
T_2^* [Spine (ms)]	20.4 ± 1.2 (W=0.95, p=0.91)*	5.5 ± 0.8 (W=0.96, p=0.92)*	14.0 ± 1.5 (W=0.79, p=0.09)*	4.9 ± 0.4 (W=0.77, p=0.07)*	t=-3.24, p<0.05	t=-1.63, p<0.05
T_2^* [Tibia (ms)]	20.6 ± 1.6 (W=0.91, p=0.56)*	10.8 ± 0.4 (W=0.89, p=0.24)*	16.5 ± 1.2 (W=0.92, p=0.64)*	9.0 ± 0.5 (W=0.85, p=0.25)*	t=-2, p<0.05	t=-2.69, p<0.05

BMD: Bone Mineral Density, vBMD: volumetric Bone Mineral Density and TrD: Trabecular Volumetric Density.

Data are mean ± standard deviation.

* For Shapiro-Wilk normality test, the statistical significance level under which the null hypothesis is rejected was set at p<0.05. According to the quoted Shapiro-Wilk normality test results, it is confirmed that the data of the present study are normally distributed.

as magnetic field inhomogeneities increased, due to the increasing concentration of the gadolinium, as expected. **(Table 3)** [26]. Clinical experiments proved the ability to measure even lower T_2^*. Therefore, in future experiments one might attempt to increase the concentration of gadolinium solutions for assessing and measuring even lower relaxation times.

The control group of this study consisted of women without bone metabolic disorders and former spine or tibia fracture with mean age 33.3 ± 10.4 years. According to the National Institutes of Health Osteoporosis and Related Bone Diseases National Resource Center (USA), the amount of bone tissue in the skeleton is thought to be increasing by around age 30. At this point, bones have reached their maximum strength and density. Women tend to experience minimal change in total bone mass between age 30 and menopause as the rate of bone turnover is considered to be stable and generally low. But in the first few years after menopause, most women go through rapid bone loss, which then slows, but continues throughout the postmenopausal years [29].

The correlations between T_2^* and BMD measurements in our study were comparable with the existed international literature. Damilakis et al. [15] demonstrated a substantial increase in T_2^* measurements of L_1–L_4 vertebrae of the lum-

bar spine in 26 postmenopausal women with osteoporotic fractures compared to 28 age-matched women without fractures (16.4 ± 3.9 ms for patients vs. 13.2 ± 3.8 ms to healthy women). BMDs of spine, hip and phalanx speed of sound (SOS) were estimated through DXA and quantitative ultrasound (QUS) examinations, respectively. There was a moderate correlation between spine T_2^* and BMDs. More precisely, r=-0.40 (p<0.01) for the region of spine and r=-0.40 (p<0.0001) for the region of hip. The same pattern observed for the phalanx r =-0.33 (p<0.05) [15]. The same research team increasing the studied cohort (38 osteoporotic and 63 healthy controls) and following the same approach found significant differences between two groups (osteoporotic group: 14.3 ± 0.9 ms; HC: 12.6 ± 0.4 ms), t=-2.19 (p<0.05) [18]. Also, there was a weak negative correlation between T_2^* and BMD, r=-0.26 (p<0.005). These results are also in line with Funke et al. which examined the T_2^* measurements of the fourth lumbar vertebra. The researchers received T_2^* relaxation times of 13.4 ms for healthy individuals and 19.9 ms for osteoporotic [16].

Wehrli et al. estimated the R_2^* rates ($\frac{1}{T_2^*}$) in the lumbar spine (L_3-L_5) of 77 healthy and 59 osteoporotic women. The estimated reported R_2^* rates were 64.8 s (T_2^*: 15.4 ms) for healthy women and 53.4 s (T_2^*: 18.4 ms) for osteoporotic. R_2^* correlated with BMD satisfactorily, r=0.54 (p<0.0001)
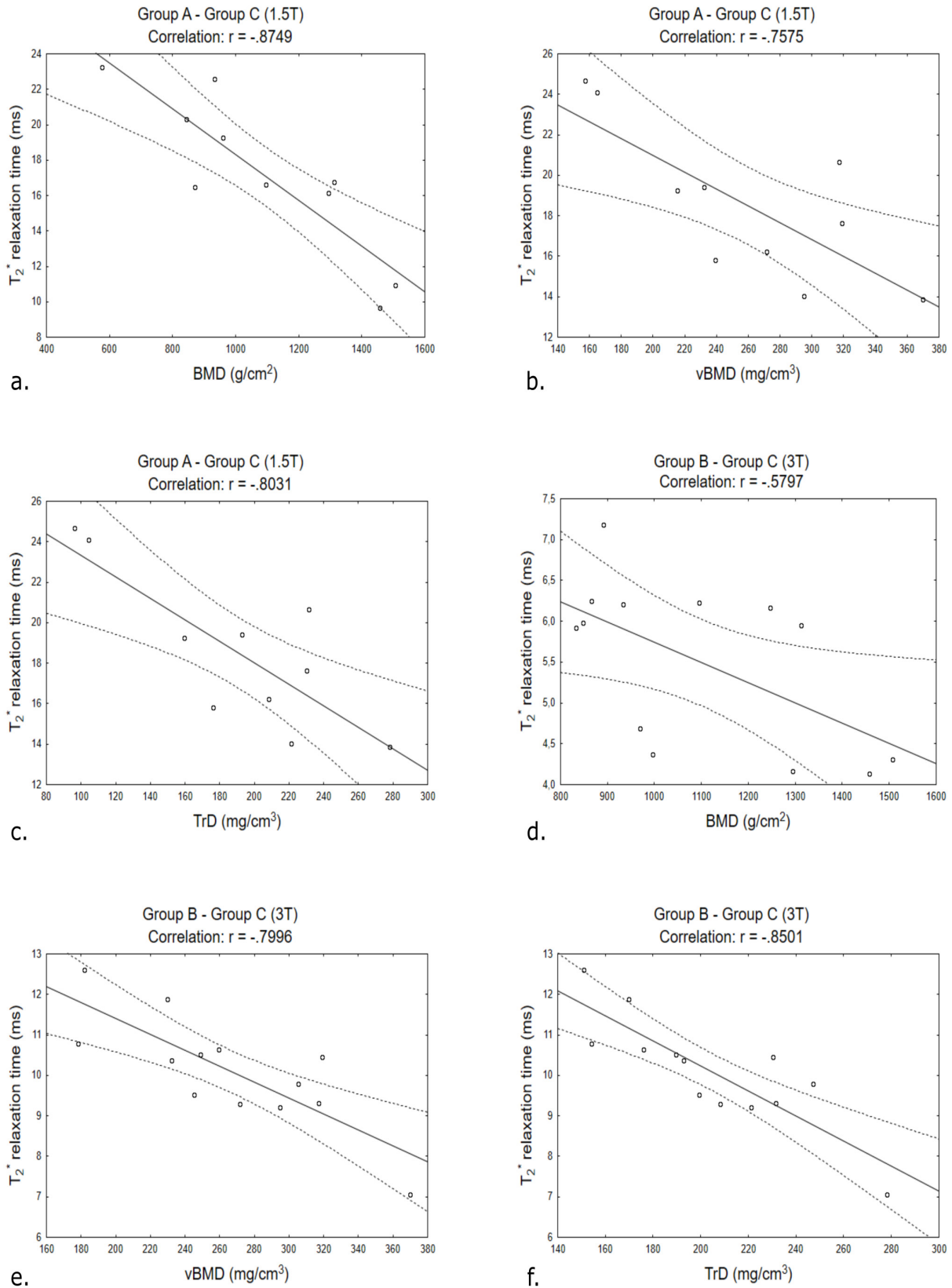
Fig. 3. Correlations between bone mineral density parameters (BMD, vBMD and TrD) and calculated T_2^* relaxation times amongst study groups. BMD vs. T_2^* on L1-L4 vertebrae, [(a) 1.5T, (d) 3.0T)]; vBMD vs. T_2^* on tibia [(b) 1.5T, (e) 3.0T)]; and TrD vs. T_2^* on tibia region [(c) 1.5T, (f) 3.0T)]. (Note 95% confidence).

[13]. Kang et al. tried to associate T_2^* of the calcaneus with BMD measurements, by DXA and QUS, from the calcaneus, spine (L_2-L_4) and femoral neck. Thirty two postmenopausal and 14 young normal (group Y) women were recruited in this research. Postmenopausal women were divided into two subgroups, group O (women with low BMD) and group N (women with normal BMD). The estimated T_2^* of the calcaneus region were 11.4 ± 1.2 ms, 11.2 ± 1.3 ms and 12.8 ± 1.5 ms for Y, N and O groups, respectively. For groups N and O, T_2^* correlated significantly with calcaneus BMD, broadband ultrasound attenuation (BUA) and SOS, r=-0.61 to -0.80 (p<0.0001 – 0.0003). However, moderate correlations were reported between calcaneus T_2^* and BMDs of spine and femoral neck. More precisely, r=-0.53 (*p*<0.002) and -0.34 (*p*<0.06), respectively [30]. Grampp et al. evaluated the association between R_2^* and DXA measurements in the trabecular bone of the distal 5 cm of the radius in 14 healthy premenopausal women, 11 healthy postmenopausal women and in 11 women with osteoporosis. TrD and total BMD were measured with pQCT. In healthy women, R_2^* and TrD at pQCT were significantly correlated, however, R_2^* and total BMD were not. Statistically significant correlations (p=0.03) between R_2^* and DXA were found only in the most distal area covered with DXA [31]. The inhomogeneity of T_2^* values in control groups among the published studies leads to the conclusion that each imaging center has to standardise their own reference control values. The available T_2^* values quoted in the literature are not comparable and cannot be used for clinical use by an independent physician mainly due to the different acquisition protocols and to be more specific, because of the different first echo and ΔTE. The signal in different TEs is strongly influenced by the chemical shift phaenomenon. The signal of the fatty bone marrow is added in in-phase and subtracted in out-phase, leading to a sinusoidal signal decay. In order to increase the validity of the calculated relaxation times, this signal modulation has to be avoided [15, 18]. In our study, ΔTE was set 2.3 ms at 3.0 T and 4.6 ms at 1.5 T to achieve only in phase or out-phase images.

The results of the present study show significant differences of T_2^* and bone density parameters between the control group and the postmenopausal groups **(Table 4)**.

The means T_2^* of both lumbar spine and tibia were lower in the control group compared to the postmenopausal groups. Also, a significant negative correlation of both lumbar spine and tibia T_2^* with subject's BMD, vBMD and TrD measurements **(Fig. 3)** was estimated compared to the above referred studies.

It is worth noting that slightly better T_2^* correlations were recorded for the region of tibia against the lumbar spine. Owing to the anatomic site of the lumbar spine there is moderate SNR and presence of more artefacts than in a tibia's lesion in bigger TEs during the MR examination. Ghosting artefacts were visible in bigger TEs due to respiratory movement and body fluids (blood flow, especially from the abdominal aorta, movement of cerebrospinal fluid) affecting negatively both SNR and image quality.

The main limitation of our study is the small number of participants. The necessity of prospective multi-centered studies with increased number of participants remains in order to lead to more valid conclusions on a statistical basis. Moreover, the absence of a phantom vial considered as a reference standard with similar T_2^* relaxation times in both 1.5 T and 3.0 T MRI scanners is an additional limitation. Nevertheless, our study is strengthened by the use of multiple approaches. DXA, pQCT and two different magnetic field MRI scanners were used to estimate the reliability of T_2^* relaxation time as a bone structural integrity index.

In conclusion, this study suggests that through the phaenomenon of magnetic resonance recovery and hence the measurement of the transverse recovery (relaxation) times, T_2^* has the potential to assess changes in bone status related to bone mineral density measurements between healthy premenopausal and osteoporotic postmenopausal women. **R**

Conflict of interest
The authors declared no conflicts of interest.

REFERENCES

1. Kanis JA, Cooper C, Rizzoli R, et al. European guidance for the diagnosis and management of osteoporosis in postmenopausal women. *Osteoporos Int* 2019; 30(1): 3-44.

2. Link TM. Osteoporosis Imaging: State of the art and advanced imaging. *Radiology* 2012; 263(1): 3-17.

3. Kanis JA. Assessment of fracture risk and its application to screening for postmenopausal osteoporosis: Synopsis of a WHO report. *Osteoporos Int* 1994; 4(6): 368-381.

4. Blake GM, Knapp KM, Spector TD, et al. Predicting the risk of fracture at any site in the skeleton: Are all bone mineral density measurement sites equally effective? *Calcif Tissue Int* 2006; 78(1): 9-17.

5. Bouxsein M. Bone quality: where do we go from here? *Osteoporos Int* 2003; 14(5): 118-127.

6. Engelke K, Glüer CC. Quality and performance measures in bone densitometry. *Osteoporos Int* 2006; 17(9): 1283-1292.

7. Hildebrand T, Laib A, Müller R, et al. Direct three-dimensional morphometric analysis of human cancellous bone: Microstructural data from spine, femur, iliac crest, and calcaneus. *J Bone Miner Res* 1999; 14(7): 1167-1174.

8. Kanis JA, Burlet N, Cooper C, et al. European guidance for the diagnosis and management of osteoporosis in postmenopausal women. *Osteoporos Int* 2008; 19(4): 399-428.

9. Ward KA, Adams JE, Hangartner TN. Recommendations for thresholds for cortical bone geometry and density measurement by peripheral quantitative computed tomography. *Calcif Tissue Int* 2005; 77(5): 275-280.

10. Davis CA, Genant HK, Dunham JS. The effects of bone on proton NMR relaxation times of surrounding liquids. *Invest Radiol* 1986; 21(6): 472-477.

11. Ford JC, Wehrli FW, Chung HW. Magnetic field distribution in models of trabecular bone. *Magn Reson Med* 1993; 30(3): 373-379.

12. Link TM, Majumdar S, Augat P, et al. Proximal femur: assessment for osteoporosis with T2* decay characteristics at MR imaging. *Radiology* 1998; 209(2): 531-536.

13. Wehrli FW, Ford JC, Haddad JG. Osteoporosis: clinical assessment with quantitative MR imaging in diagnosis. *Radiology* 1995; 196(3): 631-641.

14. Yablonskiy DA, Haacke EM. Theory of NMR signal behavior in magnetically inhomogeneous tissues: The static dephasing regime. *Magn Reson Med* 1994; 32(6): 749-763.

15. Damilakis J, Maris T, Papadokostakis G, et al. Discriminatory ability of magnetic resonance T2* measurements in a sample of postmenopausal women with low-energy fractures: A comparison with phalangeal speed of sound and Dual X-Ray Absorptiometry. *Invest Radiol* 2004; 39(11): 706-712.

16. Funke M, Bruhn H, Vosshenrich R, et al. [The determination of the T2* relaxation time for characterizing trabecular bone]. [Article in German]. *Rofo* 1994; 161(1): 58-63.

17. Jergas MD, Majumdar S, Keyak JH, et al. Relationships between young modulus of elasticity, ash density, and MRI derived effective transverse relaxation T2* in tibial specimens. *J Comput Assist Tomogr* 1995; 19(3): 472-479.

18. Maris TG, Damilakis J, Sideri L, et al. Assessment of the skeletal status by MR relaxometry techniques of the lumbar spine: comparison with dual X-ray absorptiometry. *Eur J Radiol* 2004; 50(3): 245-256.

19. Folkesson J, Goldenstein J, Carballido-Gamio J, et al. Longitudinal evaluation of the effects of alendronate on MRI bone microarchitecture in postmenopausal osteopenic women. *Bone* 2011; 48(3): 611-621.

20. Rajapakse CS, Phillips EA, Sun W, et al. Vertebral deformities and fractures are associated with MRI and pQCT measures obtained at the distal tibia and radius of postmenopausal women. *Osteoporos Int* 2014; 25(3): 973-982.

21. Stathopoulos KD, Katsimbri P, Atsali E, et al. Age-related differences of bone mass, geometry, and strength in treatment-naïve postmenopausal women. A tibia pQCT study. *J Clin Densitom* 2011; 14(1): 33-40.

22. Price R, Allison J, Clarke G, et al. 2015 American College of Radiology MRI Quality Control Manual 2015. Available via https://www.acr.org/. *Published* 2004. Updated 2015. Accessed January 22, 2020.

23. Bloembergen N, Purcell EM, Pound RV. Relaxation

effects in nuclear magnetic resonance absorption. *Phys Rev* 1948; 73(7): 679-712.

24. Jaovisidha S, Sartoris DJ, Martin EME, et al. Influence of spondylopathy on bone densitometry using Dual Energy X-Ray Absorptiometry. *Calcif Tissue Int* 1997; 60(5): 424-429.

25. Laskey MA, Crisp AJ, Compston JE, et al. Heterogeneity of spine bone density. B*r J Radiol* 1993; 66(785): 480-483.

26. Gold GE, Han E, Stainsby J, et al. Musculoskeletal MRI at 3.0 T: Relaxation times and image contrast. *AJR Am J Roentgenol* 2004; 183(2): 343-351.

27. Chung H, Wehrli FW, Williams JL, et al. Relationship between NMR transverse relaxation, trabecular bone architecture, and strength. *Proc Natl Acad Sci U S A* 1993; 90(21): 10250-10254.

28. Sebag GH, Moore SG. Effect of trabecular bone on the appearance of marrow in gradient-echo imaging of the appendicular skeleton. *Radiology* 1990; 174(3): 855-859.

29. National Institutes of Health Osteoporosis and Related Bone Diseases National Resource Center. Osteoporosis: Peak Bone Mass in Women. Available via https://www.bones.nih.gov/health-info/bone/osteoporosis/bone-mass. *Published* 2012. Updated October 1, 2018. Accessed January 22, 2020.

30. Kang C, Paley M, Ordidge R, et al. In vivo MRI measurements of bone quality in the calcaneus: A comparison with DXA and ultrasound. *Osteoporos Int* 1999; 9(1): 65-74.

31. Grampp S, Majumdar S, Jergas M, et al. Distal radius: in vivo assessment with quantitative MR imaging, peripheral quantitative CT, and dual X-ray absorptiometry. *Radiology* 1996; 198(1): 213-218.